Ab-initio simulation of doped injection layers.

Franz Symalla*, Artem Fediai**, Jonas Armleder**, Simon Kaiser**, Timo Strunk*, Tobias Neumann*, Wolfgang Wenzel**

*Nanomatch GmbH, Karlsruhe, Germany
**Karlsruhe Institute of Technology, Institute of Nanotechnology, Karlsruhe, Germany

Abstract

Optimization of doped injection layers in state-of-the-art OLEDs via experimental trial&error by tuning host-dopant combinations/concentrations is time-consuming and costly. We present a multiscale-simulation approach to investigate doping on microscopic level, i.e. the impact of microscopic properties on doping performance, and illustrate how to apply simulations towards materials design.

Author Keywords

OLED; digital twin; computer aided design; doped injection layers; predictive device simulations

1. Introduction

Doped injection layers are commonly used in state-of-the-art OLED devices with the purpose to a) lower injection barriers and b) generate free charge carriers, increasing conductivity of injection layers [1-3]. A major challenge is the material dependence of the performance of doped injection layers which complicates the optimization of material combinations and doping concentration for a specific OLED stack. Specifically, it is not understood how microscopic molecular properties of dopant and host material determine device performance, and custom-tailored development of host-dopant material combination and optimization of doping concentration for a specific purpose via trial&error fabrication, production and characterization remains a time-consuming and costly process.

Computer simulations can aid this purpose [4,5], but well-established continuum models such as drift-diffusion rely on parametric models require input e.g. from experiment, which limits their application in the development of new materials. Further, individual microscopic bimolecular processes that play a crucial role in device performance, especially in doping, are not resolved in these models.

In this study we present a review of recent progress in the the simulation and analysis of doped injection layers based on first principles, exemplified for the system alpha-NPD:F4TCNQ (N,N' -Bis(naphthalen-1-yl)-N,N' -bis(phenyl)-2,2'-dimethylbenzidine and 2,3,5,6-Tetrafluoro-7,7,8,8-tetracyanoquinodimethane).

2. Method

To enable the analysis of microscopic processes such as doping on device performance based solely on quantities derived from first principles, we follow a seamless bottom-up multiscale modeling approach. In this approach, a digital twin of the device is generated down to the electronic scale, and properties computed with quantum chemistry methods are ultimately mapped to charge transport and exciton simulations. This approach, illustrated in Figure 1, was recently applied to investigate individual aspects of OLED devices from ab-initio with reliable accuracy, such as charge carrier mobility or quenching in emission layers [6-14]. In this study, we extend the workflow and analyze fundamental principles and processes in doped injection layers, alpha-NPD doped with F4TCNQ, to extend the application of computer simulations in OLED design.
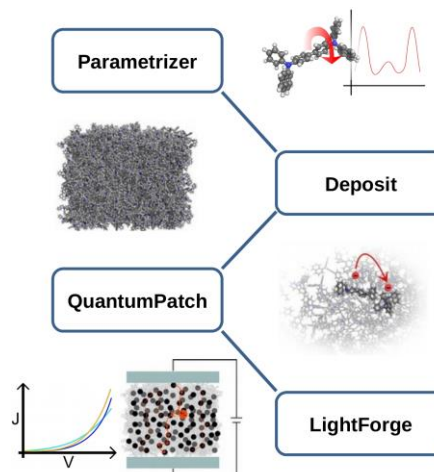

Figure 1: Multiscale workflow for ab-initio OLED simulations

Our prior studies [15,16] have shown that doping efficiency is determined by the interplay between intrinsic and doping-induced material disorder, the position of the doping induced energy levels (polaron level) and Coulomb interaction. One shortcoming in these studies is the assumption of classical Coulomb interaction between the charged molecules and a homogeneous distribution of energy levels. Here we expand this model by considering real material morphology and computing the distribution of the Coulomb interaction between dopant-host pairs as a function of their distance on a quantum-mechanical level.

This approach goes beyond recent works, where the doping activation energy has been only computed for a single dopant molecule [3]. This step is crucial and far from being trivial from computational point of view: As the strength of the Coulomb interaction in the integer charge transfer complex determines the ionization probability and the number of mobile charge carriers (that is, the doping efficiency [17]), the correct, molecular-specific, distribution of this quantity depending on the host-dopant distance is the critical parameter for *in-silico* design of the efficient dopant-host pairs.
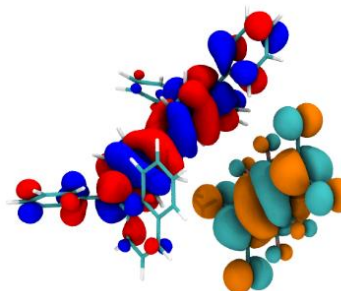

Figure 2: Orbitals of a host-dopant pair: An electron is transferred from the HOMO of the host (red/blue) to the LUMO of the dopant, creating a hole on the host.

For the analysis of the injection layer consisting of alpha-NPD doped with F4TCN we use LightForge KMC [9,12] to dynamically simulate the charge transfer between dopant and host (illustrated in Figure 2) and charge carrier dynamics. For each host-dopant pair, this charge transfer depends on the charge transfer (CT) activation energy ΔE_{act}, the energy difference between activated (Figure 3b) and neutral (Figure 3a) host-dopant pair in an uncharged environment, and an additional dynamic contribution of the coulomb interaction with charges in the vicinity. Due to systematic error in the computation of absolute energies with DFT, ΔE_{act} cannot be computed directly. Instead we compute the Coulomb binding energy of host-dopant pairs, V_C

$$V_C = \Delta E_{act} - (IP_{host} - EA_{dopant}) \qquad (1.1)$$

for which the systematic DFT error cancels out. IP of hosts (Figure 3c) and EA of dopants (Figure 3d), for which the same DFT error exist, but is to a large extend systematic are corrected separately.
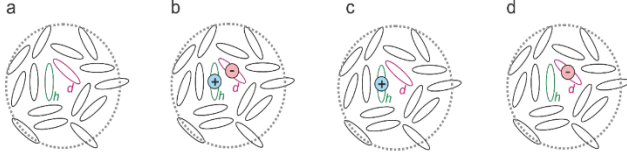

Figure 3: States of the host-dopant pair required to compute the binding energy of a dopant-host CT-state: a) neutral host-dopant pair b) activated host-dopant pair c) charged host d) charged dopant

To compute distance dependent distributions of the coulomb binding energy $V_C(r)$, as well as distributions for host IP and dopant EA energies, we virtually generated a mixed morphology (1500 molecules, 95% alpha-NPD, 5% F4TCNQ) of the doped injection layer with atomistic resolution using Deposit [18], a Monte-Carlo based simulation protocol mimicking physical vapor deposition based on customized molecular force-fields. Using QuantumPatch [6,7], V_C, IP_{host} and EA_{dopant} are computed for 50 host-dopant pairs in the morphology while taking into account the response of molecules in the environment purely on a quantum-mechanical level. In LightForge KMC we draw values of these distributions to compute the activation energy for each host-dopant pair of an extended morphology (25x25x25nm) to dynamically simulate the charge transfer process and charge carrier dynamics in the doped injection layer. Further details of this method can be found in [19].

3. Results

As explained above, we used QuantumPatch to compute energy levels of host (IP) and dopants (EA) and a distribution of the coulomb binding energy. Averaged over 50 molecules, this resulted in $IP_{host} = 5.44eV$ and $EA_{dopant} = 4.84eV$. Note that the host IP is approx. 100meV lower compared to the usual IP of alpha-NPD due to the presence of F4TCNQ in the thin film. The distance dependent distribution of the coulomb binding energy, $V_C(r)$, computed for 50 host-dopant pairs with different relative orientation, is depicted in Figure 4.

We find that most electron hole pairs are bound by up to 0.9eV, hindering CT-states dissociation. Notably, such energies at these

distances correspond to a low permittivity of approx. 2.0 in a classical model. This is in contrast to eps between 3 and 4 at larger distances usually assumed for bulk organic semiconductors. Further, we find a large spread of energies induced by different relative orientations of pairs. This spread is in line with our approach to use distribution in contrast to use single value per distance.

In addition to the coulomb-binding energy, the dissociation of an electron-hole pair after ionization of the dopant is determined by the transport levels (in the case of hole-doping the transport levels of holes (IP)) of neighboring host molecules of the surrounding host molecules. Previous studies have shown that the presence of guest molecules in organic films can shift these transport levels by up to 0.5 eV [20].
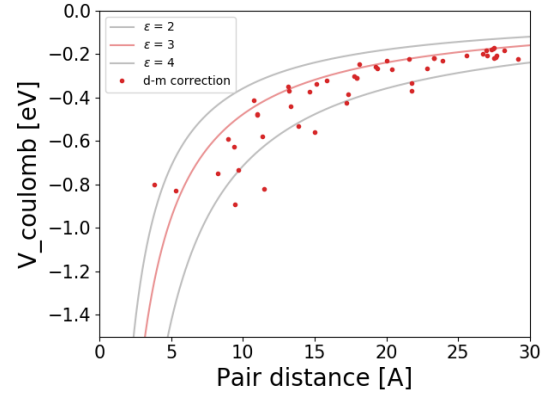

Figure 4: Coulomb binding computed for 50 host-dopant pairs in the morphology.
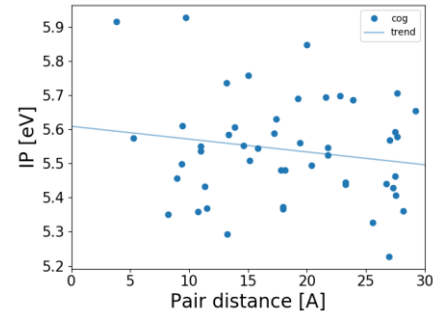

Figure 5: Distribution of host IP levels in dependence of the distance to the nearest dopant.

To estimate the impact of this effect in doped systems, we computed IP distributions of 50 molecules in an alpha-NPD morphology doped with F4TCNQ in dependence of the distance to the nearest dopant using QuantumPatch, i.e. taking into account the unique electrostatic environment of each molecule. The results are displayed in Figure 5. According to the linear fit, IP levels of host molecules near dopants are lower than the average value of -5.44eV computed above. This indicates that dopants not only globally but especially locally lower the transport levels of host molecules. This is in line with the observed increase of energetic disorder in alpha-NPD from ~100meV to ~150meV when doped. As holes tend to go up in energy, this effect partially compensates coulomb-binding energy, improving charge separation.

Using the distribution of the coulomb interaction of Figure 4 along with computed energy levels we conducted dynamic LightForge simulations to compute fraction of activated dopants, Fermi level, conductivity activation energy, number of free charge carriers and conductivity in the doped injection layer. To extract the conductivity activation energy $E_{act,c}$ we simulated the temperature dependence of the conductivity. For activated transport we observe an exponential increase of conductivity with increased temperature, as charge is thermally propelled from a bound state to the charge transport level.

$$J \propto e^{\left(E_{act,c}/k_B T\right)} \tag{1.2}$$

We determine this conductivity activation energy by measuring the slope of the conductivity versus the inverse temperature.

For disordered materials, the hole transport level $E_{transport}$ is the energy around which a transport percolation path can be established and can be defined as the difference between Fermi level and transport activation energy:

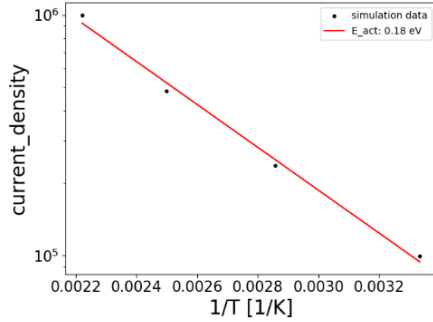$$E_{transport} = E_F - E_{act,c} \tag{1.3}$$

Figure 6: Temperature dependent computation of conductivity of alpha-NPD doped with 10% F4TCNQ results in a conductivity activation energy of 180meV.
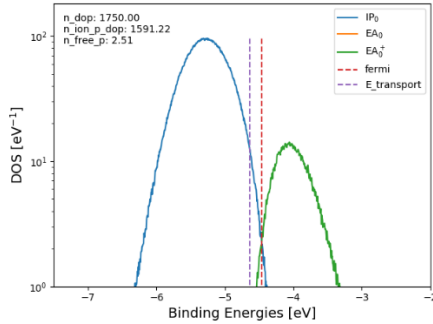

Figure 7: Density of states (DOS) of the HOMO levels of neutral host molecules (-IP) in their dynamic environment, and hole (EA_0^+) levels.

Temperature dependent conductivity in the alpha-NPD:F4TCNQ sample is depicted in Figure 6. From the slope we derive a transport activation energy of 180meV. We further computed the fraction of

activated host-dopant pairs (pairs for which a charge is transferred from dopant to host) to be 91%.

We determined the Fermi energy by extracting the energy at which hole and electron occupation probability is equal [15]. For the doped system, the hole levels are given by the IP distribution of the neutral hosts in the dynamic environment of all charges and the electron affinity distribution of the host molecule cations labeled by EA+, which corresponds to hole energies. Figure 7 shows the density of states (DOS) of alpha-NPD molecules in the doped layer. From this we derive a Fermi energy of $E_F = -4.46eV$, resulting in a charge transport energy of $E_{transport} = -4.65eV$.

The number of free charge carriers is defined as the number of all holes which occupy states below transport energy. The full method details will be published separately. In the case of alpha-NPD:F4TCNQ, we derived a total average of 2.52 free charge carriers in a sample of 25x25x25 nm^3.
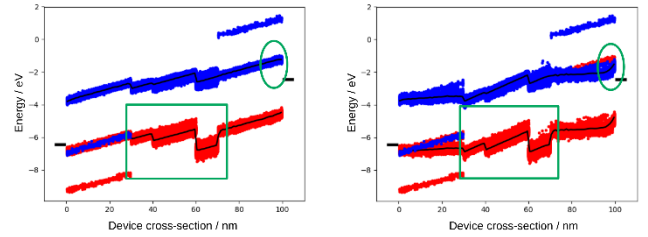

Figure 8: OLED band-diagrams to illustrate the impact of doped injection layers on device performance. Left: band-diagram before charge transfer from dopants to host molecules (before "activation"). Right: band-diagram after activation of dopants in KMC simulations. Before the activation, there is a constant voltage drop throughout the device, as expected. After activation, no voltage drop is observed in the injection layers, leading to a higher voltage drop over transport and emission layers (green box). Further, energy levels are aligned to the work function of the electrode after activation (green circle).

To illustrate the general impact of doping on full OLED device performance to motivate this study, we performed an additional KMC study of a multilayer OLED device including two doped injection layers. A digital twin of the OLED was generated using the multiscale-workflow described above including 1% dopants in the injection layers. Similar to the analysis above, charge transfer from dopants to host molecules was simulated taking into account local energetics of each host-dopant pair. The impact of this "activation" of dopants is shown in Figure 8: First, at the interface to the electrodes charge carriers generated by the charge transfer from dopant to host exit the doping layer (holes in the HIL, electrons in the EIL). The resulting net charge (negative in the HIL and positive in the EIL) pulls the energy levels of host molecules to the electrode level (fermi-level alignment), as indicated in the green circles of Figure 8. Further, upon activation of host dopant pairs there is no voltage drop along the doped injection layers, modifying the voltage drop in the inner part of the OLED (i.e. transport and emission layers). This modified voltage drop (green box in Figure 8) impacts charge carrier balance and OLED device performance. Notably, these effects are strongly material-specific as coulomb interaction and transport levels (EA and IP) determines the fraction of activated dopants.

4. Discussion/Conclusion

We investigated doping in the system alpha-NPD:F4TCNQ using LightForge KMC device simulations with input derived solely from first principles using a multiscale modeling approach. By computing distributions of coulomb binding energy, host-IP and dopant-EA with QuantumPatch on atomistic morphologies we modeled the charge transfer processes between dopant and host molecules in a digital twin of the doped injection layer. Additionally, we derived the number of free charge carriers in the system as well as the fraction of activated dopants. This computational approach can be used to complement experimental efforts in the design and optimization of organic molecules for doped injection layers, either by screening of potential candidates, or by providing microscopic insight to generate a fundamental understanding and establish structure function relationships. An example for this is the relationships between the structure of a given donor acceptor pair and the coulomb binding energy, which in turn affects the number of free charge carriers. Such structure function relationships can be used to derive design rules for material optimization. Another possible application is the optimization of dopant concentration with respect to current activation energies.

Further, we illustrated how doped injection layers impact device performance due to Fermi-level alignment at the electrodes. These results indicate that it is essential to explicitly including doped injection in full OLED device simulations to provide reliable results.

5. Acknowledgements

6. References

[1] B. Lüssem et al., *Chem. Rev.* 2016, 116, 22, 13714-13751

[2] Schwarze et al., *Nature Mater* **18,** 242–248 (2019)

[3] C. Gaul et al.,*Nature Mater* **17,** 439–444 (2018) doi:10.1038/s41563-018-0030-8

[4] P.Friederich et al., *JCTC* **2014** *10* (9), 3720-3725

[5] P. Kordt et al., *Adv. Funct. Mater.*, vol. 25, no. 13, pp. 1955–1971, Apr. 2015

[6] P. Friederich et al., *Adv. Funct. Mater.*, vol. 26, no. 31, pp. 5757–5763, Aug. 2016

[7] P. Friederich et al., *J. Chem. Theory Comput.*, vol. 10, no. 9, pp. 3720–3725, Sep. 2014.

[8] P. Friederich et al., *Chem. Mater.*, vol. 29, no. 21, pp. 9528–9535, Nov. 2017

[9] F. Symalla et al., *SID Symp. Dig. Tech. Pap.*, vol. 49, no. 1, pp. 340–342, 2018.

[10] S. Heidrich et al., adts.201900222, submitted

[11] F. Symalla et al., *Phys. Rev. Lett.*, vol. 117, no. 27, Dec. 2016

[12] F. Symalla et al., *SID Symp. Dig. of Tech. Pap.*, 50: 259-262, 2019

[13] D. Tabor et al., Chem. Sci., 2019, 10,

[14] P. Friederich et al., *Adv. Mater.* 2019, 31, 1808256.

[15] A. Fediai et al., *Nat Commun* **10,** 4547 (2019)

[16] Fediai A. et al. Disorder-driven doping activation in organic semiconductors (submitted)

[17] M. Tietze et al., *Nat Commun* **9,** 1182 (2018)

[18] T. Neumann et al., J. Comput. Chem., vol. 34 no. 31, 2013

[19] A. Fediai et al, Ab initio based multiscale simulations of amorphous doped organic semiconductors (in preparation)

[20] S. Bag, et al., *Sci Rep* **9,** 12424 (2019)